

## **Obstacle Avoidance System for Autonomous Transportation Vehicle based on Image Processing**

Eiji MORIMOTO, Masahiko SUGURI, Mikio UMEDA

Laboratory of Farm Machinery Division of Environmental Science and  
Technology Graduate School of Agriculture Kyoto University,  
Sakyo-ku Kyoto, 606-8502, JAPAN  
eiji@elam.kais.kyoto-u.ac.jp

### Abstract

The labor shortage and the aging problem of farmers are serious problem for Japanese agriculture. In order to solve those problems, this research suggested that the smart mechanization system should play an important role for food production. The Autonomous Transportation Vehicles (ATVs) has a possibility to achieve this task. ATVs was applied with a CCD camera for vehicle control (i.e. for straight running, turning and emergency stop). We reported here how to recognize an obstacle for safe running by image processing. Hue, Saturation and Intensity were applied for obstacle recognition parameters and a binary image was produced by image processing. Finally, distance information (i.e. between vehicle and obstacle) was estimated using coordinate transformation between camera coordinate and vehicle coordinate. Experiments, indicated the obstacle recognition method could detect obstacles under the both sunny and cloudy condition. The error of distance estimation was within 0.3m and its processing speed was 5.9 frame/s.

### Keywords

Obstacle Recognition, Image processing, HSI value, Coordinate transformation

### Introduction

Japanese agriculture faces several problems. The food self-sufficiency rate was only 27% (cereal base) in 1999, is the lowest among the developed countries. Also the average age of farmers has increased to more than 60 years old and, 28% of

farmers are over 65 years of age. It is clear that the number of Japanese farmer will decrease significantly with a compounding decrease in both supply.



Fig. 1 Rice farm road

In order to avoid these problems, numerous studies have been made to increase the efficiency of farming. This project was also intended to improve an effectiveness rice production.

Generally, the size of rice field is much smaller than that of European or US ones: the average size being only 0.9ha per farm. In addition, a single field may be divided into several sections by canal and farm roads as shown in Fig. 1. Since farm roads create a gap between fields, transportation vehicles and farm machinery can't pass freely, as shown in Fig. 2. Since one farmer usually has to operate one field, when farmer transports materials, farm machinery can't operate or while farmer is driving farm machinery in the field, the transportation vehicle can't work.

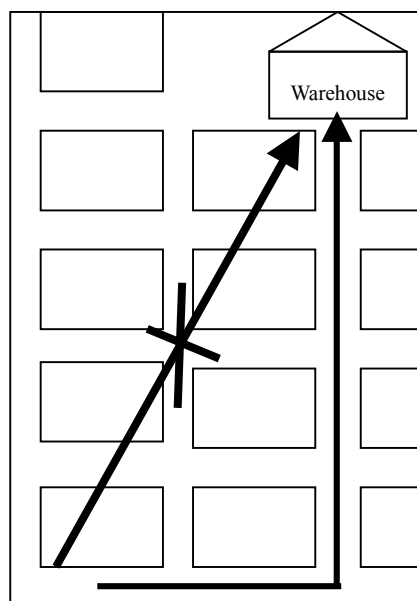


Fig. 2 Limitation of transportation route



Fig. 3 Prototype vehicle

As it was mentioned above, the unmanned transportation system has a potential to inspire the effectiveness of farming. Fig. 3 shows the prototype vehicle, whereupon a

CCD camera has been installed as an external sensor. The image information could be useful for detecting position, orientation, intersections and obstacles. This paper focused on “How to detect an obstacle?” based on the image processing. Image processing speed and error of distance estimation were used as evaluation parameters for this research.

## Material and Method

### HSI transformation and Smoothing

The following techniques were employed for obstacle recognition as shown in Fig. 4. The obstacle recognition system should search only farm roads, since the transportation vehicle could run only on the farm road. The image acquisition area was limited only to the farm road using a boundary line (between field and road) detection method Suguri et al(1999). Image data was acquired as RGB values (Red, Green and

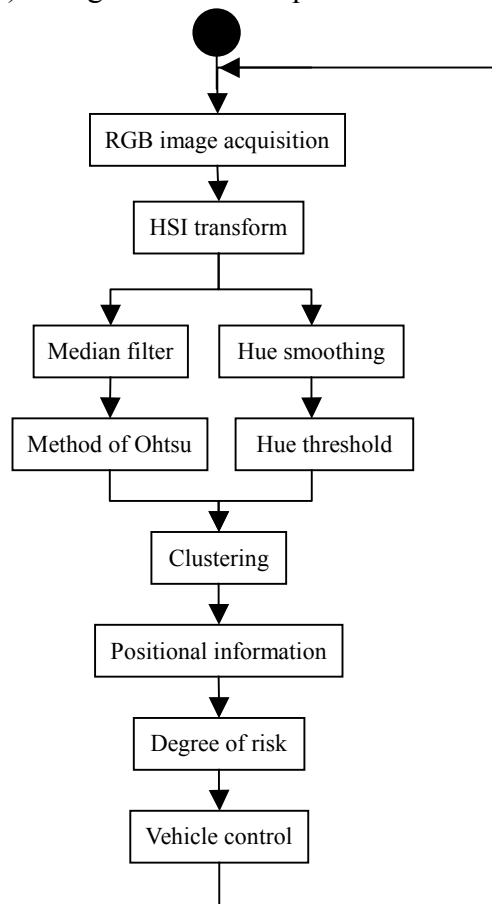


Fig. 4 Method of obstacle finding

Blue), and the image data was transformed into HSI image (Hue, Saturation and Intensity), Smith (1978) in order to use for the obstacle recognition parameter, since HSI value is not influenced as much as the RGB value under strong sunlight condition.

Median filter, Narendra (1978), was applied for Saturation and Intensity for noise reduction of original image as well as RGB image. However, Hue can't be applied in the same method as Saturation, since the characteristic of the Hue is a cyclical pattern (i.e.  $0-2\pi$ ), therefore sometimes the average of Hue value has no meaning. For instance, if we defined Red as 0, Green can be  $\pi/3$  and Blue can be  $2\pi/3$ . Then the average Red and Blue should be Green and its value is going to  $\pi/3$  (i.e. (0

$+2\pi/3)/2=\pi/3$ ). However this answer is not correct (correct answer is  $5\pi/6$ : means Purple), as is shown in Fig. 5. That is why, it was necessary to develop a smoothing algorithm called "Hue Smoothing". Hue  $\theta_n$  [rad] was transformed to the complex plane and Eq. 1 gave sum of Hue  $A_{sum}$  at the local domain (4x4 pixels).

$$A_{sum} = \sum_{n=1}^{16} \cos \theta_n + j \sin \theta_n \quad (1)$$

Also the representative value of Hue  $\theta_{ave}$  was given by Eq. 2, which related to positive and negative of  $\alpha$  and  $\beta$ .

$$\theta_{ave} = \begin{cases} a \tan(\beta / \alpha) & (\alpha > 0 \text{ and } \beta \geq 0) \\ a \tan(\beta / \alpha) + 2\pi & (\alpha > 0 \text{ and } \alpha < 0) \\ a \tan(\beta / \alpha) + \pi & (\alpha < 0) \\ \pi / 2 & (\alpha = 0 \text{ and } \beta \geq 0) \\ 3\pi / 2 & (\alpha = 0 \text{ and } \beta < 0) \end{cases} \quad (2)$$

Where  $\alpha$  is the summation of real number

$\beta$  is the summation of complex number

### Binary method

Saturation and Intensity were applied in the method of Ohtsu (1980), which defines the dynamic threshold, which we call "discriminant analysis method". A fundamental principle established for optimum threshold value from density histogram of image so that the threshold value can be known when the decentration of interclass  $\sigma B^2(k)$  came to maximum as follows in Eq. 3.

$$\sigma B^2(k) = \omega_0 (\mu_0 - \mu\tau)^2 + \omega_1 (\mu_1 - \mu\tau)^2 \quad (3)$$

where  $\omega_0 = \sum_{i=0}^k p_i$ ,  $\omega_1 = \sum_{i=k+1}^L p_i$ ,  $\mu_0 = \sum_{i=0}^k i p_i \omega_0$ ,  $\mu_1 = \sum_{i=k+1}^L i p_i \omega_1$ ,  $\mu\tau = \sum_{i=0}^L i p_i$ ,

$$p_i = \frac{n_i}{N}, \quad n_i = \text{Pixel number of level } i, \quad N = \text{Total number of pixels}$$

However, for the same reasons mentioned above, Hue could not be applied using the Method of Ohtsu; therefore a new technique was developed for dynamic Hue threshold that we call “Hue thresholding”. Fig. 5 shows an example of Hue frequency on a farm road. It was possible that the farm road had a characteristic and concentric

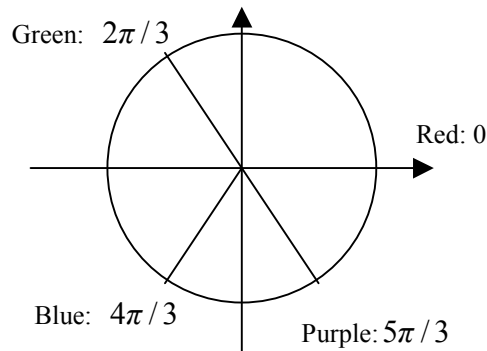


Fig.5 Hue plane

value, even in different seasons. The Hue threshold was applied for executing the Hue histogram from the original image without an obstacle, and defined the highest frequency information as its standard value. The Hue area of farm road can be estimated as follows in Eq. 4. A decision on the obstacle's Hue area, that we call “Obstacle Area” as shown in Fig. 6. In addition, this method has flexibility for Obstacle Area. Since this method detects the standard value from the next image, we can only search the present area from the previous one, and we detect the next standard value, which has nearest peak to the previous one. Thus we can make a dynamic binary image of the Hue value.

Finally we extract the obstacle area from the result of binary of Hue, Saturation and Intensity by logical multiplication.

$$\lambda_{\min} < \lambda < \lambda_{\max} \quad (4)$$

Where

$$\lambda_{\min} \text{ is } \theta_{\text{median}} - \pi/4, \quad \lambda_{\max} \text{ is } \theta_{\text{median}} + \pi/4, \quad \theta_{\text{median}} \text{ is standard value}$$

## Clustering and Distance estimation

The estimated obstacle candidate pixels usually include some noise, caused by the surface condition of the farm road. Since, the farm road was covered by grass and sometimes a different color, the road area may be detected as an obstacle. Therefore, we applied a clustering filter at a certain threshold level in order to remove small size of clusters. Finally, the extracted image was defined as an obstacle image. One of the most important parameters is the distance between the vehicle and the obstacle. In order to estimate the distance, the representative point of the obstacle was used in image plane, and representative coordinate  $(a_{rep}, b_{rep})$  was related to the minimum value of b-axis in the camera coordinate (camera coordinate a-b is set on the focal plane of the camera) as shown in Fig. 7. Fig. 8 shows the geometry of the coordinate system between image coordinate and vehicle coordinate. It is assumed that the ground is flat, the camera depression angle  $\varphi$  [rad] and the height of the camera  $z$  [mm] are constant; in addition, the camera optics can be represented by a pin hole model (without distortion); the vehicle doesn't roll and pitch. The equation of the coordinate transformation from camera coordinates to vehicle coordinates, is the following Eq. 5.

$$\begin{aligned} x &= a \cdot z / f \sin \varphi - b \cos \varphi \\ y &= z(f \cos \varphi + b \sin \varphi) / f \sin \varphi - b \cos \varphi \\ a &= fx / z \sin \varphi - y \cos \varphi \\ b &= f(y \sin \varphi - z \cos \varphi) / z \sin \varphi + y \sin \varphi \end{aligned} \quad (5)$$

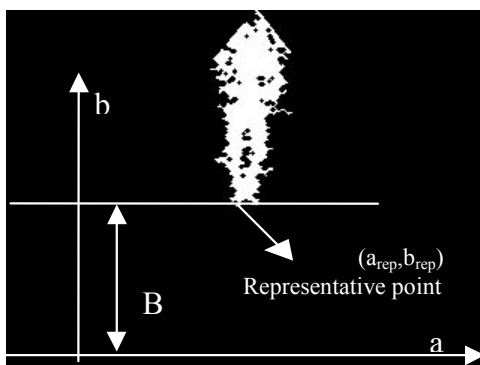


Fig. 7 Representative point

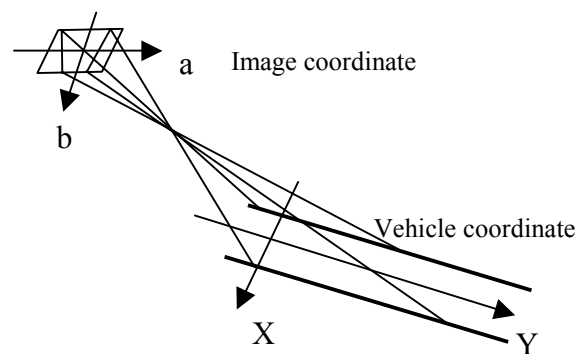


Fig. 8 Coordinate transformation between image plane and vehicle coordinate

## Result and Discussion

The obstacle detection system was evaluated by field tests at the experimental farm of Kyoto University (3.5x100m). The CCD camera was fixed 1.5m height from ground level with 15 degrees of depression angle. In this field test we applied 4 colors of wear as an obstacle (i.e. blue, black, white and beige) and the test was done in daylight during September and October 1999.

Fig. 8 shows the comparison of the dispersion of the RGB image data and the HSI image data. From this result, the range of HSI data tends to more concentric than that of RGB one. Thus we might say, HSI data is useful for distinguishing an obstacle from a farm road.

Fig. 9 describes the result of obstacle detection under different times in one day: (a) is original image which was taken at 12:00 p.m., (b) is a result at 12:00 p.m., (c) is 2:00 p.m. and (d) is 4:00 p.m. In spite of various sunlight conditions, this detection technique detected only the obstacle. Fig. 10 shows the result of obstacle recognition test under strong direct sunlight. This method also was able to find that the obstacle had two different colors (blue and black), in addition to this technique did not detect their shadows. This point might be very important, when we utilize this technique on the prototype vehicle, because under the strong sunlight, a shadow may exist around the vehicle. If this technique detects a shadow as an obstacle, the vehicle can't run because the shadow is caused by the vehicle.

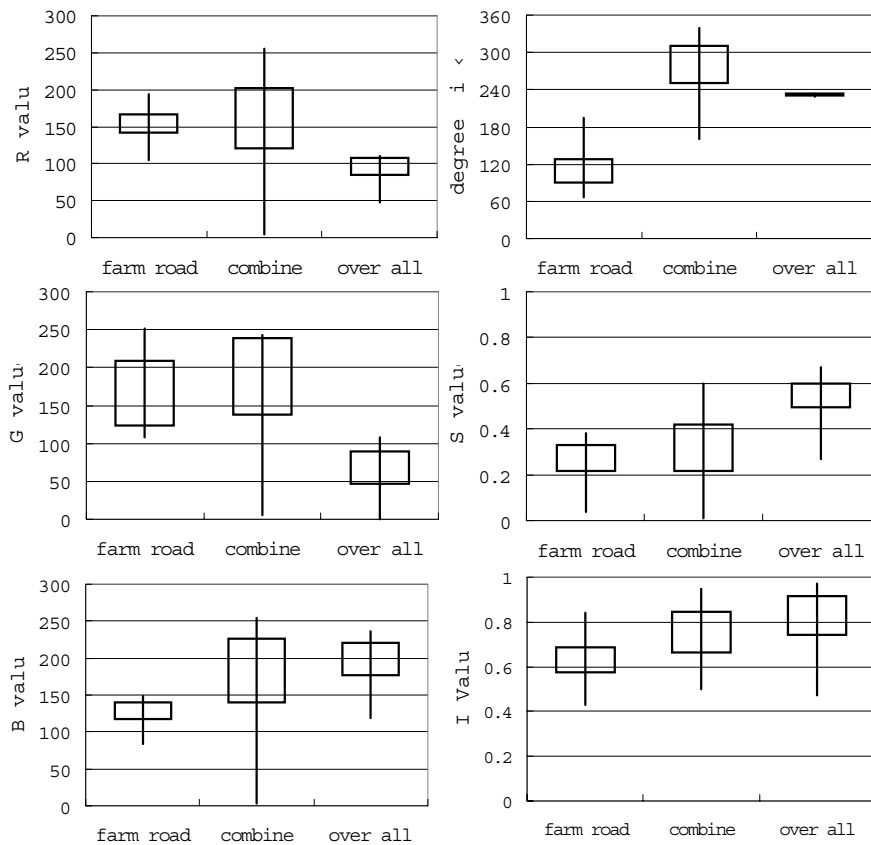


Fig.8 Comparison of RGB and HSI

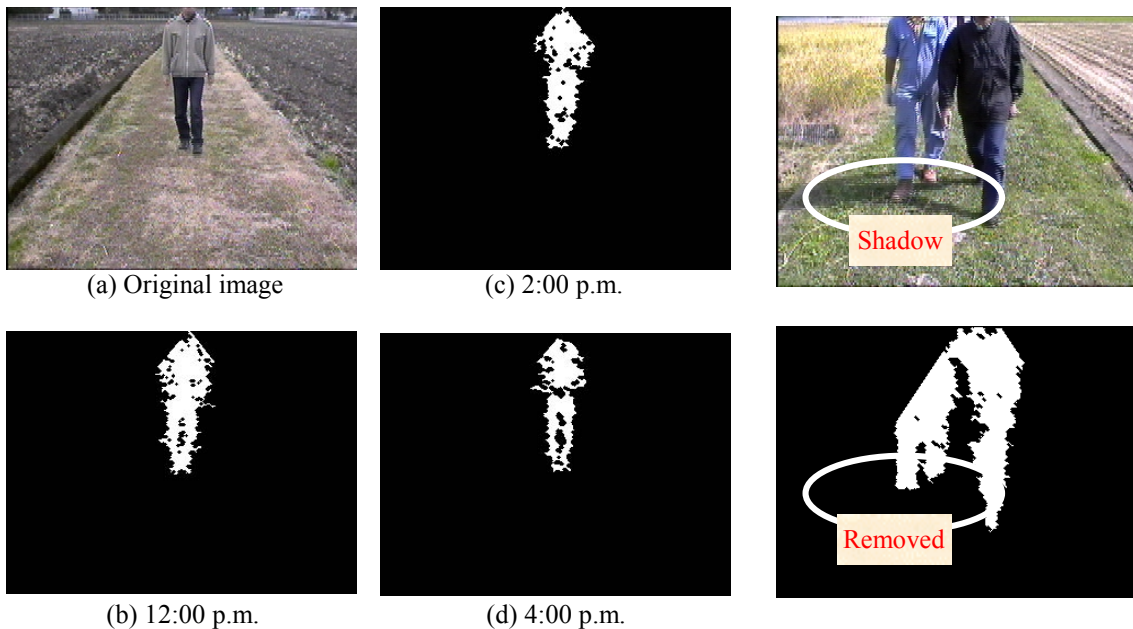


Fig. 9 Comparison of different altitude of sun

Fig. 10 Under strong sun light

However this method can ensure the effective run and we can say, Hue, Saturation  
 E. Morimoto, M. Suguri, and M. Umeda. "Obstacle Avoidance System for Autonomous  
 Transportation Vehicle based on Image Processing". Agricultural Engineering  
 International: the CIGR Journal of Scientific Research and Development. Manuscript  
 PM 01 009. Vol. IV. December, 2002.

and Intensity were useful for obstacle recognition. Also this obstacle detection method does not need to tell "What is this obstacle?", but have to tell "There is obstacle in front of the vehicle".

Fig. 11 shows a failure of obstacle detection, because the obstacle's HSI and the farm road had similar information. We might take care of our wear-color, which is not similar to farm road color information in order to distinguish easily. Fig. 12 shows the relationship between the estimated distance of the obstacle detection and hand-measured distance. The typical error was 0.3 m and the image processing speed was 5.9 Hz (Operation System FreeBSD 4.0, CPU PIII 750 MHz ). Take into account the prototype vehicle speed (0.8 m/s), this obstacle finding can process every 0.13 m interval.



Original image



Result

Fig. 11 Failure case

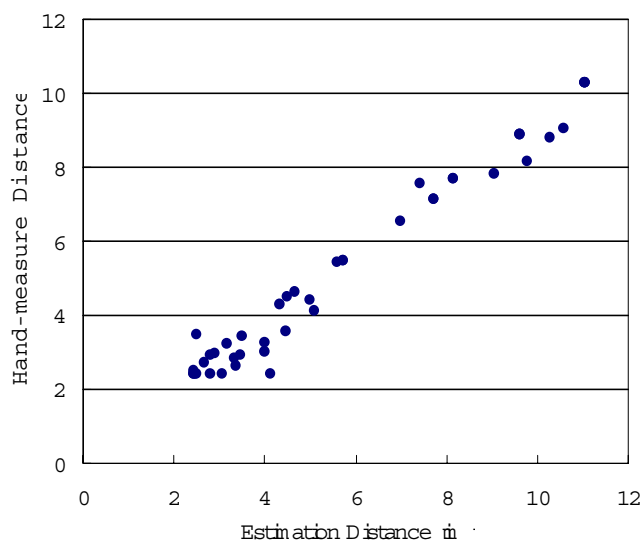


Fig. 12 Relationship between Estimate and Hand-measured distance

## Conclusion

It is possible to drive an obstacle recognition using image processing. Extracted obstacles are used as an input feature. The HSI binarization can be used to detect obstacles and distance with respect to a bottom of the obstacle pixel in camera coordinate. A developed algorithm in this research worked well when tested on numerous field experiments with five color clothes, blue, black, gray, beige and flesh color. Finally, the typical error of distance estimation was less than 0.3 m and its

image processing speed is 5.9 frame/s. Since a prototype vehicle speed is 0.8 m/s, the interval of obstacle detection is 0.13 m/time.

Additional work is necessary to detect an obstacle whose image information is similar to background/farm road.

#### Acknowledgement

The authors would like to acknowledge the financial support provided by BRAIN (BIO-oriented technology Research Advancement Institution).

#### Reference

<http://www.iga3farm.com/nougyo/jikyuritsu/>

Marchant, J.A. 1996. Tracking of row structure in three crops using image analysis, *Computers and Electronics in Agriculture*, vol.15. pp.161-179.

Narendra, P.M. 1978. A separable median filter for image noise smoothing, In *Proc. 1978 IEEE, Pattern Recognition and Image Processing*, pp.134-141.

Ohtsu, N. 1980. Discrimination and automatic adoption of threshold based on least square standard, *Transaction of The Institute of Electronics, Information and Communication Engineers*. Vol.J63-D. No.4. pp.349-356.

Smith, A.R. 1978. Color Gamut Transformation Pairs, *Computer Graphics*. vol.12. pp.12-19.

Suguri, M. Umeda, M. Morimoto, E. 1999. Path finding system for Japanese paddy field, In *Proc. 1999 ASAE/CSAE Annual International Meeting*, 99-1042. Toronto, Canada.